The population of faint Jupiter family comets near the Earth

Julio A. Fernández [a,*], Alessandro Morbidelli [b]

[a] *Departamento de Astronomía, Facultad de Ciencias, Iguá 4225, 11400 Montevideo, Uruguay*
[b] *Observatoire de la Côte d'Azur, B.P. 4229, 06034 Nice Cedex 4, France*

Abstract

We study the population of faint Jupiter family comets (JFCs) that approach the Earth (perihelion distances $q < 1.3$ AU) by applying a debiasing technique to the observed sample. We found for the debiased cumulative luminosity function (CLF) of absolute total magnitudes H_{10} a bimodal distribution in which brighter comets ($H_{10} \lesssim 9$) follow a linear relation with a steep slope $\alpha = 0.65 \pm 0.14$, while fainter comets follow a much shallower slope $\alpha = 0.25 \pm 0.06$ down to $H_{10} \sim 18$. The slope can be pushed up to $\alpha = 0.35 \pm 0.09$ if a second break in the H_{10} distribution to a much shallower slope is introduced at $H_{10} \sim 16$. We estimate a population of about 10^3 faint JFCs with $q < 1.3$ AU and $10 < H_{10} < 15$ (radii ~ 0.1–0.5 km). The shallowness of the CLF for faint near-Earth JFCs may be explained either as: (i) the source population (the scattered disk) has an equally very shallow distribution in the considered size range, or (ii) the distribution is flattened by the disintegration of small objects before that they have a chance of being observed. The fact that the slope of the magnitude distribution of the faint *active* JFCs is very similar to that found for a sample of *dormant* JFCs candidates suggests that for a surviving (i.e., not disintegrated) object, the probability of becoming dormant versus keeping some activity is roughly size independent.

© 2006 Elsevier Inc. All rights reserved.

Keywords: Comets; Photometry

1. Introduction

There has been a long debate about the existence of very small comets (sizes $\lesssim 1$ km). Of course this issue can be raised only for the Earth's neighborhood where such faint comets can be detected. Small comets can exist in huge numbers in the outer planetary region, the trans-neptunian belt or the Oort cloud, but they are beyond detection at present. Furthermore, it may be possible that the Sun's radiation generates a kind of physical barrier that prevents small comets from staying for too long in the inner planetary region without being destroyed. Kresák (1978) and Sekanina and Yeomans (1984) found no, or only very few, active comets of absolute brightness $H_{10} > 10.5$, or body diameters $D \lesssim 1$ km, among comets coming close to Earth, so these authors concluded that small active comets should be almost non-existent in the Earth's neighborhood. Furthermore, the paucity of small craters on Jupiter's moons also

suggests a dearth of comets smaller than kilometer size (Zahnle et al., 2003).

Yet, the issue of the size of the small comet population is still controversial because there is an increasing discovery number of seemingly faint, small JF comets (see, e.g., a discussion by Brandt et al., 1996). We can mention: P/1991 V1 Shoemaker–Levy 6 for which Chen and Jewitt (1994) reported an absolute nuclear magnitude $H_N = 19$, 18D/Perrine–Mrkos that disappeared after being reported to have an absolute magnitude of 19.5, 45P/Honda–Mrkos–Pajdušáková with an estimated—though quite uncertain—$H_N = 20.0$, 72P/Denning–Fujikawa and 79P/DuToit–Hartley, both with a long series of missed returns, and the latter with an estimated nuclear magnitude 18.4, and D/1978 R1 (Haneda–Campos) for which Helin and Bus (1978) reported a limiting apparent magnitude of 19.5 from prediscovery plates taken with the 122-cm Palomar Schmidt telescope, leading to an absolute nuclear magnitude $\geqslant 19.1$, or a maximum nucleus radius of 0.5 km. The near-Earth object 2003 WF$_{25}$ has been identified with the lost Comet D/1819 (Blanpain) and for it Jewitt (2006) estimates a nuclear radius

---

* Corresponding author. Fax: +598 2 525 0580.
E-mail address: julio@fisica.edu.uy (J.A. Fernández).

Table 1
Total and nuclear magnitudes of near-Earth JF comets

Comet	q_{disc} (AU)	q_{present} (AU)	H_{10}	H_N	Sources
2P/1786B1 (Encke)	0.336	0.338	9.2	16.0	1,2
3D/1772E1 (Biela)	0.990	–	7.1	–	1
5D/1846D2 (Brorsen)	0.650	–	8.3	–	1
6P/1851M1 (d'Arrest)	1.173	1.353	7.8	16.5	1,2
7P/1819L1 (Pons–Winnecke)	0.772	1.258	9.0	16.3	1,2
11P/1869W1 (Tempel–Swift–LINEAR)	1.063	1.584	11.2	–	1
15P/1886S1 (Finlay)	0.998	1.034	9.5	17.2	1,2
18D/1896X1 (Perrine–Mrkos)	1.110	–	10.0	–	1
21P/1900Y1 (Giacobini–Zinner)	0.932	1.034	9.2	17.6	1,2
24P/1911X1 (Schaumasse)	1.226	1.205	7.8	17.8	1,2
26P/1808C1 (Grigg–Skjellerup)	0.731	0.997	11.4	17.2	1,2
34D/1927D1 (Gale)	1.214	–	9.5	–	1
41P/1858J1 (Tuttle–Giacobini–Krésak)	1.140	1.052	10.4	18.4	1,2
45P/1948X1 (Honda–Mrkos–Pajdušáková)	0.559	0.528	10.8	20.0	1,2
54P/1844Q1 (deVico–Swift–LINEAR)	1.186	2.145	8.5	–	1
66P/1944K1 (duToit)	1.277	1.294	9.9	–	1
67P/1969R1 (Churyumov–Gerasimenko)	1.285	1.292	8.3	16.0	1,2
72P/1881T1 (Denning–Fujikawa)	0.725	0.780	12.6	–	
73P/1930J1 (Schwassmann–Wachmann 3)	1.011	0.937	10.6	17.7	1,2
79P/1945G1 (duToit–Hartley)	1.250	1.199	11.3	17.2	1,2
85P/1975A1 (Boethin)	1.094	1.114	7.8	–	1
103P/1986E2 (Hartley 2)	0.952	1.032	8.6	17.2	1,2
141P/1994P1 (Machholz 2)	0.753	0.749	11.7	17.5	3
D/1819W1 (Blanpain)	0.892	–	8.3	–	1
D/1884O1 (Barnard 1)	1.279	–	8.2	–	1
D/1894F1 (Denning)	1.147	–	10.0	–	1
D/1895Q1 (Swift)	1.298	–	10.7	–	1
D/1978R1 (Haneda–Campos)	1.101	–	11.4	–	1
P/1999RO28 (LONEOS)	1.232	–	15.4	22.7	4
P/2000G1 (LINEAR)	1.003	–	16.0	–	5
P/2001J1 (NEAT)	0.937	–	12.2	18.5	6
P/2001MD7 (LINEAR)	1.254	–	9.0	–	7
P/2001Q2 (Petriew)	0.946	–	10.4	–	8
P/2001WF2 (LONEOS)	0.976	–	13.7	19.6	9
P/2002O5 (NEAT)	1.174	–	14.2	–	10
P/2002T1 (LINEAR)	1.192	–	14.9	–	11
P/2003K2 (Christensen)	0.556	–	11.0	–	12
P/2003KV2 (LINEAR)	1.062	–	13.0	–	13
P/2003O3 (LINEAR)	1.257	–	13.8	–	14
P/2004CB (LINEAR)	0.912	–	14.1	–	15
P/2004R1 (McNaught)	0.988	–	14.2	–	16
162P/2004TU12 (Siding Spring)	1.228	–	12.2	–	17
P/2004X1 (LINEAR)	0.784	–	14.3	–	18

Sources: (1) Kresák and Kresáková (1989, 1994); (2) Tancredi et al. (2006); (3) IAUCs 6053, 6054, 7231, MPEC 1994-Q06; (4) IAUC 7253, MPEC 1999-R23; (5) IAUCs 7396, 7408; (6) IAUC 7623, MPEC 2001-K43; (7) MPEC 2001-N27; (8) IAUCs 7686, 7688, MPEC 2001-Q31; (9) IAUC 7827, MPEC 2001-W42; (10) IAUCs 7942, 7945, MPEC 2002-P06; (11) IAUC 7983, MPEC 2002-T15; (12) IAUC 8136, MPEC 2003-K43; (13) IAUC 8139, MPEC 2003-K53; (14) IAUC 8174, MPEC 2003-P25; (15) IAUC 8314, MPEC 2004-F96; (16) IAUC 8400, MPECs 2004-R24, 2004-R31; (17) IAUC 8436, MPECs 2004-V75, 2004-W16; (18) IAUC 8449, MPECs 2004-Y17, 2004-Y55, 2005-A51.

of only about 160 m. Several recent survey programs like LINEAR, LONEOS, NEAT, Catalina and Siding Spring, are adding a fast-growing list of potential small comets with $H_N > 18.5$ (see the references list at the bottom of Table 1). Most of these faint comets were discovered when they approached the Earth to less than a few tenths AU.

The derivation of the nucleus radius from the absolute nuclear magnitude requires the knowledge of the nucleus's geometric albedo p_v. They are related through the equation (e.g., Fernández, 2005)

$$H_N = 14.11 - 5\log R_N - 2.5\log p_v, \tag{1}$$

where the values of p_v derived for a selected set of well-observed comets are in all cases very low, with an average $p_v \simeq 0.04$ (Lamy et al., 2004). In the following we will adopt this albedo when converting the absolute nuclear magnitude to comet size.

2. Discovery rate of JF comets and NEAs

The discovery rate of near-Earth asteroids (NEAs) in cometary orbits (defined as those with aphelion distances $Q > 4.5$ AU) show a fast increase in the last few years (Fig. 1). In comparison, the discovery rate of near-Earth Jupiter family
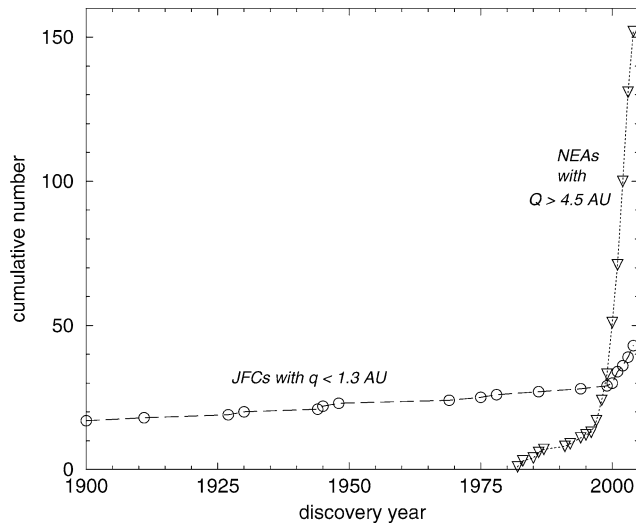
Fig. 1. The discovery rate of JF comets with $q < 1.3$ AU (circles) and of NEAs with $Q > 4.5$ AU (triangles) during the period 1900–2004.

comets (NEJFCs), defined as those with perihelion distances $q < 1.3$ AU, does not show such a sharp increase. This in itself is a strong indication that comets may not be so abundant as asteroids in the Earth's neighborhood, and this difference may increase for smaller objects ($D \lesssim 1$ km) where most of the discoveries are taking place. But, given that the discovery conditions of JF comets are somewhat different from those of NEAs, the subject requires a closer examination.

Table 1 shows the list of those comets whose perihelion distances q_{disc} were smaller than 1.3 AU at the moment of their discovery. As we can see, a few of them have increased their q above 1.3 AU, so they no longer belong to the category of NEJFC. On the other hand, 46P/Wirtanen that had $q > 1.3$ AU at discovery, has decreased it below this limit at present. The fact that JF comets rise or decrease their q's over short time scales is a consequence of their fast dynamical evolution under the gravitational influence of Jupiter. There are other JF comets that are considered extinct at present, they are designated with the prefix "D." The magnitudes H_{10} were taken from Kresák and Kresáková (1989, 1994) and from the Minor Planet Circulars and IAU Circulars for comets discovered since 1994, and they are also shown in Table 1 together with the nuclear magnitudes of the NEJFCs that have reliable estimates.

3. The relationship between total and nuclear magnitudes

The absolute total magnitude H_T of a comet roughly measures its activity (namely, the production rate of gas and dust). It is given by a relation of the kind

$$H_T = m_T - 5 \log \Delta - 2.5 n \log r, \tag{2}$$

where m_T is the apparent total magnitude, Δ is the geocentric distance (in AU), and r the heliocentric distance (in AU). The index n gives the variation of the comet brightness with the heliocentric distance. It varies from comet to comet, though an average $\langle n \rangle = 4$ is usually adopted which leads to the definition of H_{10}, namely the absolute magnitude H_T obtained for an in-

dex $n = 4$. A discussion of Eq. (2) and the index n in terms of the thermodynamic properties of the nucleus was presented by, e.g., Whipple (1978) and Meisel and Morris (1982).

The values of H_{10} derived for distant comets are always very uncertain, since the extrapolation of their apparent magnitude obtained at $r \gg 1$ AU to a heliocentric distance $r = 1$ AU strongly depends on n. Another problem is that short-period comets show complex lightcurves with indices above the average $n = 4$ (Whipple, 1978; Ferrín, 2005). Fortunately, we want to study comets that come close to the Sun ($q < 1.3$ AU), so their total brightness can be measured at r close to 1 AU, thus avoiding large and very uncertain extrapolations. Finally, we should mention that total magnitudes have been derived by means of quite different techniques. In early times most total magnitudes were measured by amateurs using the naked eye, while at present most total magnitudes are measured from CCD images. Ferrín (2005) has found that the naked-eye magnitude system is practically identical with the unfiltered CCD or CCD V magnitude system, while in the case of CCD R magnitudes, the classical $V - R = 0.5$ correction is applied. On the other hand, Kresák and Kresáková (1989, 1994) prescribe some magnitude corrections for comets fainter than $m_T = 9$ (see below).

Fernández et al. (1999) (from now on F99) found that the nuclear and total magnitudes follow a linear relation of the kind

$$H_T = a + b H_N, \tag{3}$$

where a, b are constants. For active comets close to the Sun, whose coma diameter is set by the field of view of the instrument employed, F99 found $b = 0.75$, while for low-active comets, where the limit of the coma is set by its fading into the sky background, they obtained $b = 1.5$.

Actually, H_T will depend not only on H_N (i.e., the nucleus size), but also on the fraction of active surface area f. F99 found that the total brightness $B_T \propto f R_N^{3/2}$ (valid for active comets close to the Sun), whereas the nuclear brightness $B_N \propto R_N^2$. Bearing in mind that the magnitude m is related to the brightness B through the relation: $m = k - 2.5 \log B$, where k is a constant, we get

$$H_T = a + b H_N - 2.5 \log f. \tag{4}$$

We see that a variation of f by a factor of ten causes a variation of H_T of 2.5 magnitudes.

Most of the JF comets discovered recently close to the Sun (and, in most cases, close to the Earth) are very faint, and in some cases nearly stellar. For these comets the coma diameter is set by its fading into the sky background. In this regard, Kresák and Kresáková (1989, 1994) noted that the raw observed total magnitudes must be corrected for comets fainter than apparent total magnitude $m_T = 9$, since they are taken from photographic (and more recently CCD) images that tend to record only the nuclear condensation, casting away the broader coma as part of the sky background. These authors suggested the following correction formula for the apparent total magnitude

$$m_{T,c} = 0.5 m_T + 4.5, \quad \text{for } m_T \geqslant 9, \tag{5}$$

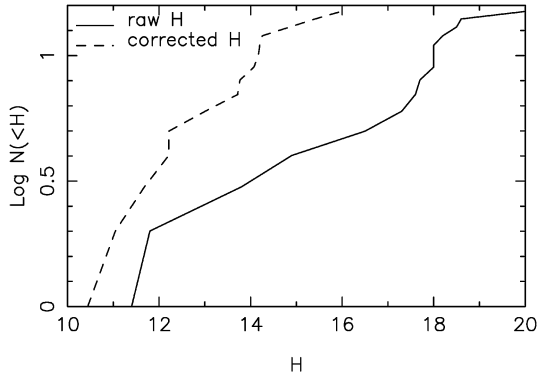where $m_{T,c}$ is the corrected apparent total magnitude.

Fig. 2. The cumulative H_{10} distributions of faint JFCs, in the cases where the absolute magnitude is computed from the uncorrected total magnitude m_T (solid curve) or the corrected $m_{T,c}$ (dashed curve).

Fig. 3. Absolute total magnitudes H_{10} versus absolute nuclear magnitudes H_N of JFCs with $q < 1.5$ AU. The solid line is the linear fit to the sample. The dashed lines represent shifts of a factor of ten in the fraction of active area.

To what extent Kresák and Kresáková's (1989, 1994) correction can be applied to every faint comet, in a time when observations are systematically done with CCD cameras, is still arguable. We notice that, if this correction is not applied and the raw m_T values are used in Eq. (2) to compute H_{10}, the resulting H_{10} distribution of the faint comets shows a sharp increase in the range 17–19 (see Fig. 2). This increase is suspicious, given that the sample should become more and more incomplete as H_{10} increases. Thus, any exponential absolute magnitude distribution would fail to fit this 'observed' distribution. Conversely, if the values of $m_{T,c}$ are used in Eq. (2) to compute H_{10}, the resulting H_{10} distribution gently bends as H_{10} increases, as expected due to the increasing incompleteness of the sample. Thus, in the following, whenever the observed m_T is fainter than 9, we use the values of $m_{T,c}$ to compute H_{10} through Eq. (2).

With the correction prescribed by Eq. (5), our sample of comets should approach to the "active-comet" regime ($b = 0.75$ in Eq. (3)), since what Eq. (5) does is to "restore" the coma lost in the sky background.

Fig. 3 plots H_{10} versus H_N for the sample of NEJFCs of Table 1, plus those with $1.3 < q \leqslant 1.5$ AU for which we have values of both H_N and H_{10}. The linear fit to the plotted values has a slope 0.90 ± 0.20, which is somewhat higher than, but still in acceptable agreement with the theoretical slope for active comets. The large scatter of points around the linear fit is probably due not only to uncertainties in the measured magnitudes, but also to the different fractions of active surface area f. The latter may play an even more important role in the scattering of points in the parametric plane H_N vs H_{10}. If the linear fit falls close to comets with $f \simeq 0.1$, the dashed lines shifted by ± 2.5 magnitudes should correspond to comets with $f = 1$ (above), or $f = 0.01$ (below).

4. The CLF for nuclear and total magnitudes

The better photometric coverage of JF comets over their whole orbits, even near aphelion where they usually are inactive, together with HST observations and a few close-up images from spacecrafts, have allowe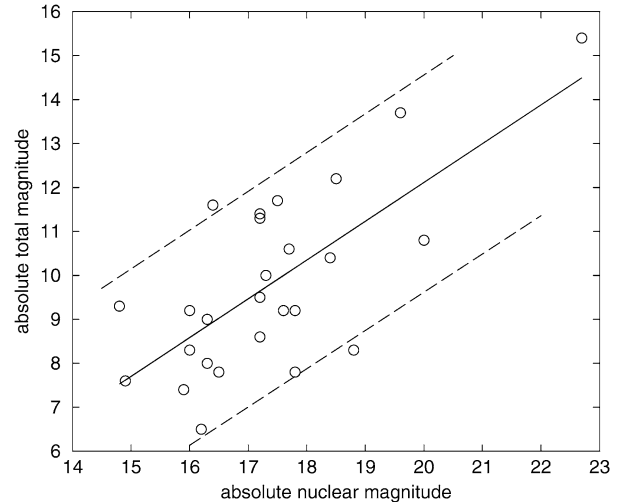d to collect a reliable database of absolute nuclear magnitudes H_N (e.g., F99, Lamy et al., 2004; Tancredi et al., 2000, 2006). From the data set of nuclear magnitudes, it has been possible to derive a cumulative luminosity function (CLF) for the JFC population. The derived CLFs are necessarily uncertain, given the smallness of the sample, though all of them satisfy a linear relation of the type

$$\log[N_N(H_N)] = C + \gamma H_N, \qquad (6)$$

where C is a constant.

The main disagreement among the different authors has to do with the value of the slope γ. For instance Tancredi et al. (2006) find a slope $\gamma = 0.54 \pm 0.05$, which holds up to $H_N \sim 16.7$ (or nucleus radii $R_N \gtrsim 1.5$ km). This CLF translates into a cumulative size distribution (CSD) of index $s = 5\gamma = -2.70 \pm 0.25$. However, other authors have obtained flatter distributions, for instance Weissman and Lowry (2003) found $s = -1.59$, Meech et al. (2004): $s = -1.45$, Lamy et al. (2004) $s = -1.66$, while Toth (2006) suggests $s = -2.0$ from the reanalysis of all the studies. The value $s = -2.0$ is in agreement with that found by Pan and Sari (2005) for the collisional evolution of gravity-dominated bodies of negligible strength. This should be applicable to bodies with sizes smaller than $\sim$40 km and larger than a few tenths km when material strength dominates gravity, i.e., within the range of cometary sizes. Yet these collisional models can only give the size distribution of comets in their source region, but do not tell anything about further evolutionary effects when comets approach the Sun, like sublimation and splittings. Tancredi et al. (2006) have explained the discrepancies in the derived values of s in terms of biases in the studied samples, the different weights given to the brightest members of the samples, and a few large differences in the computed nuclear magnitudes. In the following we will adopt Tancredi et al.'s (2006) value, but bearing in mind that it is still quite uncertain, and in particular smaller s values (in absolute terms) may be possible.

The discovery probability is better related to the total magnitude than the nuclear magnitude, so we will turn to the former.
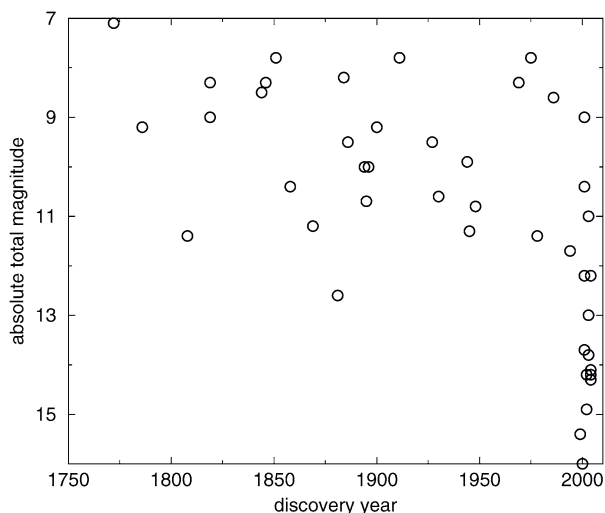
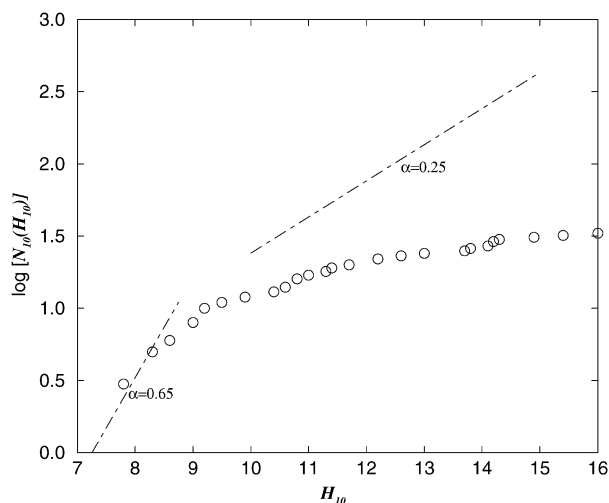Fig. 4. The absolute total magnitudes H_{10} of near-Earth JF comets as a function of the discovery date.

Fig. 5. The cumulative distribution of absolute total magnitudes of NEJFCs. Open circles are for the observed JFCs that have at present $q < 1.3$ AU. The straight lines with slopes 0.65 and 0.25 are the best-fit curves for bright and faint comets for an assumed total NEJFC population $= 430$ for magnitudes $H_{10} < 15$.

Fig. 4 shows the H_{10} magnitudes versus the discovery year. We can see that most of the recent discoveries of NEJFCs correspond to faint comets ($H_{10} \gtrsim 10$), which suggests that the sample of brighter NEJFCs is essentially complete. New bright members should mainly arise from JF comets that decrease their q below 1.3 AU.

Fig. 5 shows the CLF for the sample of total magnitudes of NEJFCs of Table 1. The linear fit is for comets with $H_{10} < 9$. JFCs with $q < 1.3$ AU that are by now considered extinct, and JFCs that have now $q > 1.3$ AU but had $q < 1.3$ AU at the moment of their discovery, were also included in the list of NEJFCs shown in Table 1 in order to have a larger sample. To test the reliability of the fit, we have also analyzed the extended sample of JFCs with perihelion distances up to $q = 1.5$ AU. We have obtained consistent results with the different samples, which can

be expressed as

$$\log\left[N_{10}(H_{10})\right] = C_1 + \alpha H_{10}, \qquad (7)$$

where C_1 is a constant. We find for the slope a value $\alpha = 0.65 \pm 0.14$, which can be considered valid for JFCs brighter than $H_{10} \simeq 9$. The uncertainty of the slope arises from the different values obtained from the different samples (namely, those obtained by changing the limiting q or the value of H_{10} where the curve starts to flatten. We have also applied the standard bootstrap method (Press et al., 1992, pp. 686–687) that generates fictitious samples of N data points by randomly drawing data points with replacement at every instance from the observed sample of N data points. Our computed value of the slope α is in fairly good agreement with that found by Hughes (2002) of $\alpha = 0.62$ for a sample of short-period comets with $q < 1.5$ AU.

We can derive a value of α from the CLF of H_N given by Eq. (6), and from the relation between H_N and H_T given by Eq. (3), from where we get

$$\log\left[N_{10}(H_{10})\right] = C_2 + \frac{\gamma}{b} H_{10}, \qquad (8)$$

where C_2 is a constant. By comparing Eqs. (7) and (8) we get $\alpha = \gamma/b$. Taking Tancredi et al.'s value $\gamma = 0.54$ and $b = 0.90$ we obtain $\alpha = 0.60$, which is consistent with the empirical value of Eq. (7).

The cumulative number of NEJFCs starts to flatten for $H_{10} \gtrsim 9$. To what extent this is due to incompleteness of the sample of discovered faint NEJFCs, or to an intrinsic scarcity of faint, small JF comets is a matter that we will address next.

5. Debiasing the orbital and H_{10}-distribution of the faint JFCs

Determining the H_{10}-distribution of faint objects is a difficult task because observational biases penalize the discovery of faint objects. The observed H_{10}-distributions are therefore always shallower than the real ones. We therefore need a way to estimate the observational biases.

The debiasing of an observed population is always problematic. In principle it requires that a large number of detections is done by a well-characterized survey, namely a survey for which the pointing history is known, as well as the limiting magnitude of each exposure (see Jedicke et al., 2002, for a review). Then, from this information, the observational bias for a body with a given orbit and absolute magnitude can be computed as the probability of being in the field of view of the survey, with an apparent magnitude brighter than the limit of detection. Assuming a distribution of angular orbital elements (typically, but not necessarily, a uniform one), the bias is a function $B(a, e, i, H)$, dependent only on semimajor axis, eccentricity, inclination and on the absolute magnitude H. Once the survey's bias is known, the real number of objects N can be estimated as

$$N(a, e, i, H) = n(a, e, i, H)/B(a, e, i, H), \qquad (9)$$

where $n(a, e, i, H)$ is the number of objects detected by the survey. This procedure has been used, for instance in Jedicke and

Metcalfe (1998) for main belt asteroids and Stuart (2001) for NEAs.

If the number of detections is small, so that the function $n(a, e, i, H)$ is equal to zero in most (a, e, i, H)-cells, the bias function can still be used, provided that one has a parametric distribution model $M(a, e, i, H, \vec{\alpha})$ of the population under examination, $\vec{\alpha}$ representing the vector of parameters. In this case, one can define a biased model by the product

$$m(a, e, i, H, \vec{\alpha}) = M(a, e, i, H, \vec{\alpha}) \times B(a, e, i, H) \qquad (10)$$

and determine the values of the parameters $\vec{\alpha}$ by best-fitting the observed distribution $n(a, e, i, H)$ with $m(a, e, i, H, \vec{\alpha})$. This procedure has been used, for instance, in Bottke et al. (2000, 2002) for the NEAs.

If the discoveries of the population's objects have been done by a collection of non-characterized surveys, the methods above cannot be applied. Some sort of debiasing can still be done, though. A possibility is to do a relative debiasing of one population relative to another one. This has been done, for instance, in Morbidelli et al. (2003) to compare the H-distributions of asteroid families relative to those of the local background populations. This requires, however, that the populations in consideration have similar orbital elements (a, e, i), cover the same range in H, and that the bias in absolute magnitude is not very sensitive on the orbital elements.

In the case of the faint JFCs, none of the approaches above can be followed. These objects have been discovered by a collection of non-characterized surveys, at least for what concerns cometary detections. In addition, there is no other population with similar orbital elements and the same absolute magnitudes that we can compare with.

Thus, should we conclude that debiasing the observed magnitude distribution of the faint comets is hopeless? Fortunately not. A new possibility is opened by a method originally introduced by Trujillo and Brown (2001) for the trans-neptunian objects discovered on the ecliptic at opposition (see Morbidelli and Brown, 2004, for a more detailed description), but that we generalize here for objects discovered at any ecliptic latitude and longitude. In essence, this is how the method works. Each observation indicates that an object has been detected at a specific latitude and longitude in the sky and a specific apparent magnitude. Given a population distribution model $M(a, e, i, H)$, one can compute the sub-distribution of the population that can be seen at that set of latitude, longitude and apparent magnitude. For each observation, therefore, one selects a model sub-distribution, namely a sub-set of the original model distribution that is consistent with the detection circumstance. A *necessary* condition for the model to be correct is that the sum of these sub-distributions gives an (a, e, i, H)-distribution that is in reasonable agreement with the (a, e, i, H)-distribution of the observed objects. In case the model depends on parameters, the values of the parameters can be determined so that this necessary condition is best fulfilled. We stress this agreement between observed and model (a, e, i, H)-distributions is only a necessary condition for the validity of the model, not a sufficient one. This is because this method does not consider the observations when no detections occurred. The information on

the list of fields and limiting magnitudes with no detections, unfortunately, is unavailable. If we had this information, possibly we could reject models because they would predict detections where instead no detections occurred. Thus, the Trujillo and Brown debiasing method is inferior to the rigorous debiasing method described above for well-characterized surveys. But in absence of well-characterized surveys, it still allows us to obtain useful information. For instance, Trujillo and Brown (2001) first showed with this method that the Kuiper belt has an edge at ∼50 AU. Later, well characterized surveys (Allen et al., 2001, 2002), just confirmed this result.

In the following we apply our generalization of the Trujillo–Brown method to debias the H_{10} distribution of faint JFCs. In Section 5.1 we detail on the construction of our parametric model. In Section 5.2 we present the list of observations that we use for the debiasing method. Section 5.3 formalizes what described above concerning the generalized Trujillo and Brown's method and details our computation of the observational biases.

5.1. The model for the 'true' distribution

To define our model we use the sample of observed bright JFCs with $q < 1.3$ AU and $H_{10} < 10$ in the following way. Let $N(=19)$ be the number of observed bright comets of Table 1. We note that a and q are somewhat correlated, while i can be considered independent of a and q. We then build a list of $N \times N$ values of a, q, i by combining every set (a, q) with every i of the N bright comets. To each one of these values we associate a set of J values of H_{10} between 10 and 21—which is the range of magnitudes of the faint comets that we are interested to—with steps of 0.5 magnitudes. Then, to each one of these $N \times N \times J$ sets of a, q, i, H_{10} we associate a 'weight,' which represents the true number of comets in each magnitude bin, namely

$$N'_{10}(H_{10}) = A \times 10^{(\alpha' H_{10})}, \qquad (11)$$

where A is a constant for the normalization of the resulting distribution and α' is a free parameter (we will test values from 0.1 to 0.5). This collection of 'weights' for all the considered values of a, q, i, H_{10} constitutes our model $M(a, q, i, H_{10})$.

Concerning the angular variables l, ω, Ω, (mean anomaly, argument of perihelion, longitude of ascending node, respectively) we assume that the population of objects in each (a, q, i, H_{10}) bin has a uniform distribution in Ω and l in the interval $(0, 2\pi)$, whereas ω follows a sinusoidal law, as observed for bright comets, with maxima around 0 and π, and minima around $\pi/2$ and $3/2\pi$ (Fernández, 2005).

5.2. The list of detected faint objects

We consider the sample of faint comets tabulated in Table 2. We have selected all NEJFCs with $H_{10} > 10$ discovered in the last ten years (1994–2004). Table 2 brings the discovery date, the apparent total magnitude m_T at discovery, and the orbital elements. We obtain the absolute total magnitudes H_{10} of these comets correcting first m_T by means of Eq. (5) and

Table 2
Faint near-Earth JF comets discovered since 1994

Comet	Discovery date	q_{disc} (AU)	e	ω	Ω	i	m_T
141P/1994P1-A (Mach. 2)	1994 08 13.42	0.752	0.75024	149.26	246.18	12.79	9.2
P/1999RO28 (LONEOS)	1999 09 7.33	1.232	0.65064	219.86	148.45	8.19	18.2
P/2000G1 (LINEAR)	2000 04 7.45	1.003	0.67236	343.29	191.03	10.37	17.0
P/2001J1 (NEAT)	2001 05 11.25	0.937	0.75833	271.03	200.79	10.16	17.6
P/2001Q2 (Petriew)	2001 08 18.42	0.946	0.69625	181.90	214.11	13.94	11.0
P/2001WF2 (LONEOS)	2001 11 17.27	0.976	0.66673	51.35	75.13	16.92	17.6
P/2002O5 (NEAT)	2002 07 30.25	1.174	0.59745	15.31	282.21	20.40	16.0
P/2002T1 (LINEAR)	2002 10 3.25	1.192	0.66376	1.31	15.50	20.71	15.2
P/2003K2 (Christensen)	2003 05 26.18	0.556	0.84062	346.65	93.55	10.15	14.6
P/2003KV2 (LINEAR)	2003 05 23.16	1.062	0.62667	188.79	66.48	25.50	17.6
P/2003O3 (LINEAR)	2003 07 30.39	1.257	0.63956	0.662	342.11	8.58	17.8
P/2004CB (LINEAR)	2004 02 3.40	0.912	0.68940	149.66	66.49	19.15	18.0
P/2004R1 (McNaught)	2004 09 6.13	0.988	0.67898	0.573	296.13	4.87	17.6
162P/2004TU12 (S. Spring)	2004 10 10.55	1.228	0.59728	356.36	31.25	27.84	14.4
P/2004X1 (LINEAR)	2004 12 7.08	0.784	0.73729	345.94	6.83	5.17	15.6

then using Eq. (2). These objects provide a list of detection circumstances $V_{\text{disc}}(k)$, $L_{\text{disc}}(k)$, $\lambda_{\text{disc}}(k)$, the index k running over the set of considered faint comets $(1, \ldots, K)$ and V, L, λ denoting respectively the apparent (total) magnitude, the ecliptic latitude and the ecliptic longitude measured from opposition. We note that $V_{\text{disc}} \equiv m_T$ of Table 2. On the other hand, the detected faint objects provide an observed a, q, i, H_{10} distribution $O(a, q, i, H_{10})$, that the biased model should correctly reproduce.

5.3. The computation of the bias function

The way to understand the debiasing procedure is to consider each faint comet as a pointer to a fictitious survey, which looked at magnitude V_{disc}, at latitude L_{disc} and longitude from opposition λ_{disc}, and found exactly one object. Let us consider one of these surveys, say that corresponding to the kth faint comet. For any set of parameters a, q, i and H_{10} spanned by our model, we compute the fraction of the population in the (a, q, i, H_{10})-bin that would be discovered by the survey. This is the fraction of the population that, given the distribution of l, ω, and Ω described in Section 5.1, satisfies simultaneously the conditions below for V, L and λ

$$V_{\text{disc}} - \delta V < V < V_{\text{disc}} + \delta V,$$

$$L_{\text{disc}} - \delta L < L < L_{\text{disc}} + \delta L,$$

$$\lambda_{\text{disc}} - \delta \lambda < \lambda < \lambda_{\text{disc}} + \delta \lambda.$$

(We have used $\delta V = \delta L = \delta \lambda = 0.001$, but this has no practical influence, provided that these values are small and fixed for all values (a, q, i, H_{10}) and for all k.)

We denote this fraction by B_k. It can be considered as the bias of survey k for objects with the considered parameters a, q, i, H_{10}. By construction, B_k is a function of (a, q, i, H_{10}).

We now define

$$m_k(a, q, i, H_{10}) = M(a, q, i, H_{10}) \times B_k(a, q, i, H_{10}) \qquad (12)$$

for all the sets of values a, q, i, H_{10} spanned by our model. The 'function' $m_k(a, q, i, H_{10})$ represents the model biased by survey k. In other words it is the model sub-population that can

be detected by survey k. Given that survey k discovered one object, m_k is normalized to unity.

Finally, we repeat the procedure for all the K fictitious surveys (i.e., one for every faint comet of our sample). Because each fictitious survey discovered the same number of objects (one each), the overall orbital-magnitude distribution of the objects discovered by all surveys is then simply

$$m(a, q, i, H_{10}) = \frac{1}{K} \sum_{k=1}^{K} m_k(a, q, i, H_{10}). \qquad (13)$$

The function m describes our ultimate model-biased distribution, to be compared with the observed distribution $O(a, q, i, H_{10})$.

6. The results

We first compare visually the observed H_{10} distribution of the selected JFCs with the distribution expected from our model $m(a, q, i, H_{10})$, for different values of α', once the observational biases are taken into account as previously explained (Fig. 6). For a better visual comparison, we plot in the figure the cumulative distributions. It is evident from the figures that a much better match is obtained with α' equal to 0.2 or 0.3 than for 0.1 or 0.4. If $\alpha' = 0.1$, the model predicts too many bright objects (the median H_{10} for the biased model distribution is 12, whereas that for the observed distribution is 14). If $\alpha' = 0.4$, the model predicts the detection of a significant fraction of comets with $H_{10} > 16$ (35%), whereas no comets beyond this magnitude have yet been observed. The lack of detections of objects with $H_{10} > 16$, therefore, sets a constraint on the H_{10} distribution of the very faint JFCs. In fact, despite of their faint intrinsic luminosity, if these comets were sufficiently numerous, some would have had the chance to pass sufficiently close to the Earth to be detected by the existing surveys. This never happened, which sets an upper bound on the number of these bodies.

In order to find the value of α' that gives the best match of the *differential* magnitude distributions (the H_{10}-distributions of the biased model and of the observed population) we use
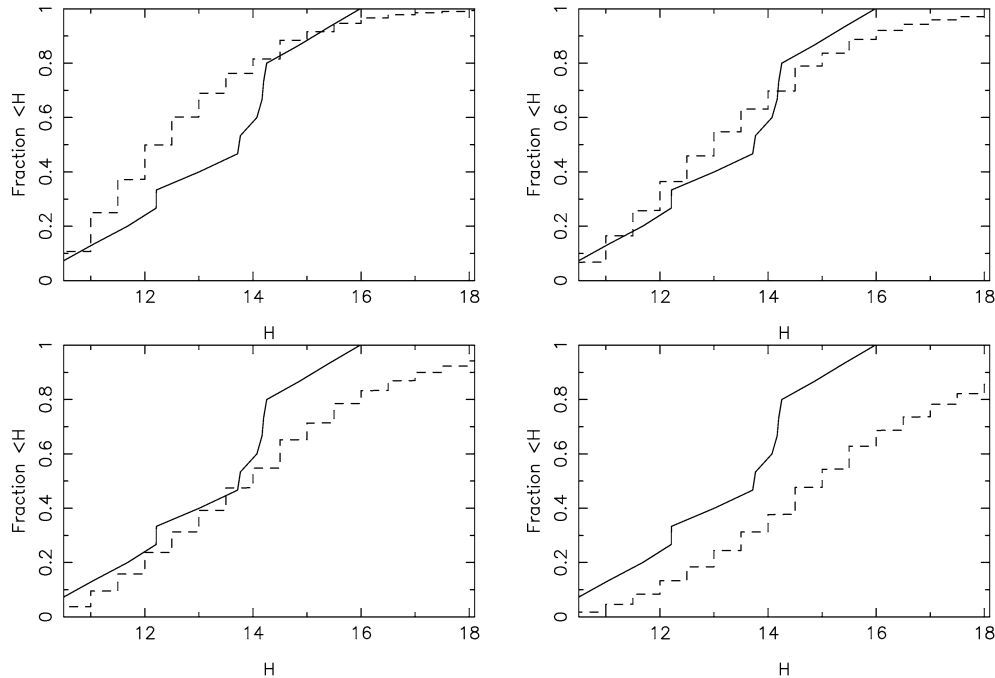
Fig. 6. Comparison between the observed H_{10} distribution of faint JFCs (solid curve) with that predicted by our model with $\alpha' = 0.1$ (top left), 0.2 (top right), 0.3 (bottom left) and 0.4 (bottom right) in Eq. (11). The model distribution has been biased as explained in the text (cf. Eq. (13)).
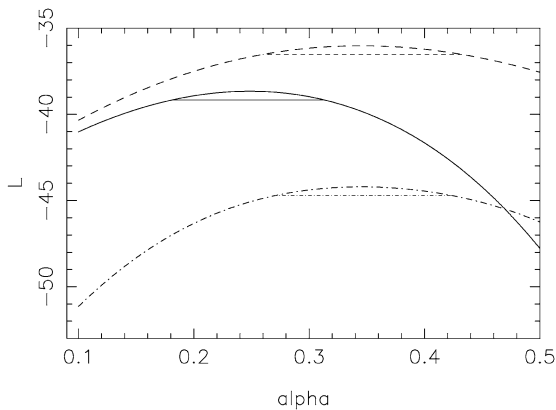

Fig. 7. The probability function $\mathcal{L}$ as a function of α', obtained from Eq. (A.2) when comparing the H_{10}-distribution of our biased model(s) and of the observed comets. The solid curve concerns the model with a unique exponent α' in Eq. (11), in the range $10 < H_{10} < 21$. The dashed curve concerns a two-slope model with exponent α' in the range $10 < H_{10} < 16$ and $\alpha' = 0$ for $H_{10} > 16$. The dashed-dotted curve concerns again a unique exponent model, but the correction of Eq. (5) on the apparent total magnitudes has not been applied to the observations and in the biasing procedure.

a rigorous optimization procedure, known as the Maximum–Likelihood (ML) method (Lyons, 1986). The ML method determines the parameter(s) of the fit that maximizes the probability that the model matches the data as described by a function $\mathcal{L}(\alpha')$ (see Appendix A).

In Fig. 7 the solid bold curve shows $\mathcal{L}$ as a function of α. The best fit value of the exponent of the magnitude distribution of Eq. (11) is $\alpha' = 0.25$, which corresponds to the maximum of $\mathcal{L}(\alpha)$ as explained in Appendix A. The horizontal thin solid line shows the value $\mathcal{L}_{max} - 1/2$. It intersects the curve at $\alpha' = 0.19$

and $\alpha' = 0.31$. Thus, the error on the best fit exponent of the magnitude distribution is $\sigma = \pm 0.06$.

Given that comets with $H_{10} > 16$ have never been discovered, we have also tried to fit the observed H_{10}-distribution with a two-slope model. This model still has the form of Eq. (11), but a different value of α' holds for $10 < H_{10} < 16$ and for $H_{10} > 16$. We have considered in particular the extreme case where $\alpha' = 0$ for $H_{10} > 16$. In this case the exponent α' in the range of H_{10} 10–16 is the only parameter of the model. The dashed curve in Fig. 7 shows $\mathcal{L}(\alpha)$ in this case. The best fit value of the exponent of the magnitude distribution is now $\alpha' = 0.345 \pm 0.09$. Thus, we conclude that in a two-slope model, the first exponent of the H_{10}-distribution can be pushed up relative to the one-slope model, considered above. Notice that the $\mathcal{L}_{max}$ is larger in the latter case than in the former case, which means that the one-slope model fits the observations better. This is not surprising, given that the fit is searched over a narrower interval of magnitudes (from 10 to 16 instead from 10 to 21).

For completeness, we have also tried to fit the absolute magnitude distribution of the observed comets that one would obtain if the correction of Eq. (5) on the apparent magnitudes is not applied. We remind that the non-application of this correction shifts the H_{10}-distribution of the observed comets as indicated in Fig. 2. If one adopts the uncorrected H_{10}-distribution, and neglects the correction of Eq. (5) also in the algorithm for the computation of the biases, the resulting function $\mathcal{L}(\alpha)$ is that shown by the dashed-dotted curve in Fig. 7. In this case the best fit value of the exponent of the magnitude distribution is $\alpha' = 0.345 \pm 0.07$. Notice however that the value of $\mathcal{L}_{max}$ is lower than those obtained in the previous two attempts, which means that the overall quality of the fit is worse. This
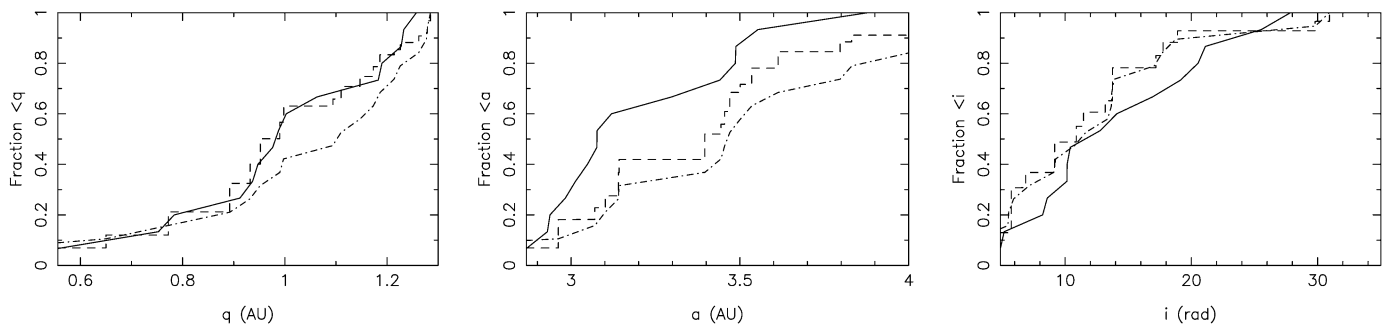
Fig. 8. The three panels show the distributions of perihelion distance (q), semimajor axis (a) and inclination (i) for the observed cumulative distribution (solid curve), our model distribution (dashed–dotted curve), and the distribution obtained once observational biases are taken into account (dashed histogram). For the computation of the biased model, a slope $\alpha' = 0.25$ in the H_{10} distribution given by Eq. (11) has been assumed, in agreement with the best-match case in Fig. 7.

is expected, given the weird shape of the uncorrected H_{10}-distribution of the observed comets shown in Fig. 2. As we explained in Section 3, we think that the correction of Eq. (5) on the apparent total magnitude is appropriate, so that we consider this result as non-pertinent to our problem.

Finally, as a sanity check, we compare in Fig. 8 the observed and predicted orbital distributions of JFCs in the case of our preferred model (the one-slope model with $\alpha' = 0.25$ and H_{10} from 10 to 21). A priori, there is no reason that the model matches the observed (a, q, i) distribution. By construction, our model depends on a unique parameter (α'), whose value is optimized to match the H_{10} distribution only. The q-distribution is a frank success. The model distribution (dashed-dotted curve) is somewhat skewed towards larger perihelion distances with respect to the observed distribution. But, once the observational biases are taken into account (dashed histogram) the model distribution matches very nicely the observations. The same is not true for the a distribution. Here, again, the model distribution is skewed towards larger values with respect to the observed distribution. Accounting for the biases partially corrects for this, but not enough, so that the biased model distribution still does not match the observation. We do not have an explanation for this mismatch. Notice, however, that the semimajor axis scale spans only 1 AU so that the mismatch is in reality only a matter of 0.1–0.2 AU. We think that, given the limited number of comets used to build the orbital distribution model (19) and of those in the faint JFC sample (15), a mismatch of 0.2 AU should not be a big concern. Finally, the model i-distribution is essentially unaffected by the observational biases (the dashed and dashed-dotted curves basically overlap), and the observed distribution is slightly skewed towards larger inclinations. The median inclinations in the observed and biased model distribution, however, are within $1°$.

6.1. The total number of small active JFCs

From the debiased H_{10} distribution found before we can compute the population of faint comets that approach the Earth down to magnitude $H_{10} \sim 15$ (that roughly corresponds to a nucleus radius $R_N \sim 0.1$ km). We start assuming that the population of JFCs with $q < 1.3$ AU is complete down to $H_{10} = 9$. There are 12 JFCs discovered with initial $q < 1.3$ AU, from which 4 are considered by now extinct and one has increased q

above 1.3 AU whereas another that had $q > 1.3$ AU at discovery has now become NEJFC, so that we have a current number of active comets with $H_{10} \leqslant 9$, $N_{10}(9) = 8$. If we assumed that the number of JFCs down to $H_{10} = 15$ followed the same law as the bright ones ($H_{10} < 9$), with a slope $\alpha = 0.65$, then the number would rise to

$$\log N_{10}(15) - \log N_{10}(9) = \alpha \times 6 = 3.9,$$
$$N_{10}(15) = N_{10}(9) \times 10^{3.9} = 8 \times 10^{3.9} \simeq 63{,}500.$$

However, as we have shown above, the H_{10} distribution becomes shallower for fainter comets. The exponent of the magnitude distribution is $\alpha' \simeq 0.25$ for $H_{10} \gtrsim 10$, or possibly $\alpha' \simeq 0.35$ if the distribution is truncated at $H_{10} = 16$. In the range $9 < H_{10} < 10$ the distribution probably starts to bend over. Given that $N_{10}(9) = 8$, if the slope remained equal to 0.65, one would have

$$N_{10}(10) = N_{10}(9) \times 10^{0.65} \simeq 35.$$

If the slope were already equal to 0.25, one would have instead

$$N_{10}(10) = N_{10}(9) \times 10^{0.25} \simeq 14.$$

Therefore we assume that $N_{10}(10) = 24 \pm 10$. Assuming now $\alpha' = 0.25$ we get

$$N'_{10}(15) = N_{10}(10) \times 10^{1.25} \simeq 430,$$

whereas assuming $\alpha' = 0.35$ we would get

$$N'_{10}(15) = N_{10}(10) \times 10^{1.75} \simeq 1350.$$

Given the uncertitude of 50% on $N_{10}(10)$, we conclude that the total number of JFCs brighter than $H_{10} = 15$ is between a few hundreds and a couple of thousands with a most likely value at $\sim 10^3$. This number is almost 2 orders of magnitude smaller than that expected if the steep magnitude distribution observed in the range 7–8.5 applied up to $H_{10} = 15$.

6.2. Comparison with the small comet population contributing to the cratering rate of Jupiter's moons

Our best-fit slope $\alpha' = 0.25$ translates into an exponent $s = 5\alpha' = -1.25$ for the cumulative size distribution of our small comet sample. From crater counts on Europa, Zahnle et

al. (2003) derived an exponent $s = -0.9$ for comets with diameters $D < 1$ km colliding with the moon, i.e., somewhat flatter, but still quite close to our CSD. Of course we should not expect to have an absolute correspondence between the small comet population colliding with Jupiter's moons and that approaching the Sun to $q < 1.3$ AU, because the latter population is affected by solar radiation (sublimation, splittings) in such a way that it may change the CSD.

6.3. Comparison with dormant JFC distribution

We can compare the population of NEJFCs with that of near-Earth objects (NEOs) in the same size range. Bottke et al. (2002) estimate a population of 960 ± 120 NEOs with $H < 18$ (that roughly correspond to diameters $D > 1$ km). This number was later upgraded to 1200 to match the discovery rate of LINEAR (Bottke et al., 2004). For this population, Bottke et al. (2000) found for the CSD a power law of index $s = -1.75$. Extrapolating the population of NEOs down to $R = 0.1$ km we find a number 20,000. If Bottke et al. estimate that about 6% of NEOs with $R > 0.5$ km are dormant JFCs, held to $R \sim 0.1$ km, then the number of dormant JFCs larger than this size limit would be 1200. Assuming that $H_{10} = 15$ corresponds to the same nuclear size $R \sim 0.1$ km, we conclude that the ratio between the number of dormant and active JFCs would be about 1–3. Levison and Duncan (1997) estimated from dynamical considerations that this ratio should be between 2 and 6.7.

In terms of the physical evolution of cometary nuclei, the computed ratio dormant/active $\simeq$ 1–3 tells us that a comet nucleus may spend in the dormant state a time about 1–3 times longer than that in the active state during its stay in the Earth's neighborhood. This result can be compared with that found by Fernández et al. (2002) of an upper limit of ~ 0.4 for the ratio dormant/active based on dynamical considerations. Again, given the uncertainties in several of the quantities introduced here, this discrepancy cannot be considered as very serious.

The exponent of the absolute magnitude distribution of dormant NEJFCs has been recently evaluated by Whitman et al. (2006). They found $\alpha' = 0.3 \pm 0.03$, slowly decreasing towards 0.2 when a more restrictive sample—less contaminated by asteroids—is taken into account. Their value of α' in principle cannot be directly compared to ours, because they considered nuclear absolute magnitudes H_N (their considered objects do not show any cometary activity) while we considered in this paper the total absolute magnitude H_{10} (nucleus plus coma). However, as shown in Fig. 3, there is a roughly linear average relationship between H_N and H_{10}, with slope 0.9. This means that the slopes of the H_N distribution and of the H_{10} distribution can be directly compared. The result by Whitman et al. holds for $16 < H_N < 21$, which roughly corresponds to $9 < H_{10} < 13$ (see Fig. 3) so that their work and our work concern dormant and active JFCs in the same size range.

Our result together with that of Whitman et al. (2006) shows that the absolute magnitude distributions (and hence the size distributions) of active and dormant JFCs are about the same. This suggests that the probability of becoming dormant versus keeping some activity should be roughly size independent so

that the slope of the distribution is preserved. Whitman et al. did a careful job in selecting the dormant comet candidates, but their selection criterion is nevertheless model-dependent. Thus, we caution that, if a substantial fraction of the putative small dormant comets in Whitman et al. turn out to be *bona fide* asteroids, the conclusion on the similarity of the size distributions of active and dormant NEJFCs would have to be revised.

The fact that both the distributions of active and dormant JFCs are shallow suggest two possibilities. The first one is that the source of JFCs (the scattered disk) has an equally shallow size distribution. This is not implausible, because the scattered disk preserve a fraction of the population of planetesimals initially in the protoplanetary disk through which the giant planets migrated. Thus, although the current collisional activity inside the scattered disk is minimal, originally the comets had to belong to a massive small body population which could be at collisional equilibrium. It is now known that, because the impact strength of the planetesimals is size dependent and has a minimum at about 100 m in radius (Benz and Asphaug, 1999), the equilibrium size distribution is very shallow in the range 100 m–5 km. In fact, according to the SDSS survey (Ivezić et al., 2001) the main asteroid belt (the best example we have of a small body reservoir in collisional equilibrium), has an H-distribution with $\alpha \sim 0.26$ in the range between 300 m and 5 km in diameter.

The second possibility is that as comet precursors start to penetrate into the Centaur region they start to suffer strong thermal stresses. These stresses might induce a size-dependent disintegration before the objects become 'comets,' which makes the size distribution of the surviving objects much shallower than that of the parent reservoir. On the other hand, larger comets (radii $\gtrsim 1$ km) may better withstand solar radiation as they can develop insulating dust mantles (e.g., Rickman et al., 1990) that preserve them in the Sun's neighborhood for longer time scales. This may explain the bimodality in the magnitude (size) distribution of NEJFCs shown in Fig. 5.

It is yet not possible to discriminate between the two possibilities outlined before on the origin of the shallow size distribution of NEJFCs. To do it we would need information on the size distribution in the scattered disk, which might be achieved by observing the crater distribution on trans-neptunian objects during future rendez-vous missions.

In the inner planetary region, some small comets (diameters $\lesssim 1$ km) will show gaseous activity if they still have volatile material available, so they will be classified as comets. Yet, it is possible that most small comets will have exhausted their volatile content, so they will look inactive and be classified as "NEOs." These small comets may be a mixture of primordial small bodies plus the remains of larger parent comets and fragments of comet breakups. A good example of these highly eroded, or fragments of parent comets, that are by now inactive or very low active, is the NEO 2003 WY$_{25}$, identified with the lost Comet D/1819 W1 (Blanpain), for which Jewitt (2006) detected coma activity and estimated a nucleus radius of only ~ 160 m. We should expect for these small bodies very short physical lifetimes, as they will continue their disintegration process into meteoritic dust, so most of them will fade away

before being observed, thus explaining their scarcity and the consequent flattening of the CLF for $H_{10} \gtrsim 9$. Again, the similarity of the size distributions of active and inactive objects (if confirmed) indicates that the probability of being active or inactive, or of evolving from one category to the other, must be roughly size-independent.

7. Concluding remarks

The debiasing method applied to the sample of discovered faint NEJFCs allows us to derive a CLF with a slope 0.25 ± 0.06 (or at most 0.35 ± 0.09, if a second bending towards an even shallower slope beyond $H_{10} = 16$ is accepted). This result suggests that the CLF of faint comets is much flatter than the CLF derived for brighter comets under most reasonable assumptions. The bending occurs at $H_{10} \sim 9$–10.

Thus, the fact that we get a CLF with two different slopes: $\alpha = 0.65$ for comets brighter than $H_{10} \sim 9$, and $\alpha = 0.25$ for NEJFCs fainter than $H_{10} \sim 10$, has important consequences in the total number of small (faint) comets: the population decreases from about 6×10^4, if the slope were $\alpha = 0.65$ all the way to $H_{10} = 15$, to about 400–1300 if the CLF has a bimodal distribution. Therefore, the population of small comets turns out to be much smaller (about one percent) than that expected from a straightforward extrapolation of the CLF of bright comets.

The slope of the magnitude distribution that we have found is very similar to that of dormant JFCs (Whitman et al., 2006). Why are both distributions so similar and so shallow? We can advance two possible explanations: either (i) the source population of JFCs has an equally shallow distribution and a size-independent fraction of active JFCs become dormant or (ii) there is a size-dependent decimation by disruption in the transport process from the trans-neptunian to the JFC region; and the objects that survive this decimation then have a size-independent probability of becoming dormant versus keeping some activity.

Acknowledgment

Appendix A

We illustrate the ML method for a normalized function $F(x, \alpha)$, where in our case F represents our biased model for the magnitude distribution, the variable x represents the magnitude H_{10}, and α is the free parameter (called α' in Eq. (11)). The function F represents the probability that an 'event' (i.e., an observation) corresponding to a given value of x can occur, according to the model. If there are n events with $x = x_i$ $(i = 1, n)$, then the probability of obtaining those n events is obviously proportional to:

$$L(\alpha) = \prod_{i=1}^{n} F(x_i, \alpha). \tag{A.1}$$

Maximizing L with respect to α provides the value of α that best matches the model with the observations.

For the purpose of maximizing Eq. (A.1), it is beneficial to take its logarithm to convert the product into a sum. Maximizing the logarithm of a function is equivalent to maximizing the function itself. The function then becomes

$$\mathcal{L} = \ln(L) = \sum_{i=1}^{n} \ln\big[F(x_i, \alpha)\big]. \tag{A.2}$$

The value of α when $\mathcal{L}$ is at its maximum ($\mathcal{L}_{\max}$) provides the best fit of the model to the data.

In the ML method, the statistical error on the most probable result is found by obtaining the values of α at $\mathcal{L}_{\max} - 1/2$ on both the positive and negative sides of $\alpha(\mathcal{L}_{\max})$. This can be easily shown as follows. In a Gaussian distribution $y = \exp(-x^2/2\sigma^2)$, so at $x = \sigma$ we have $y = \exp(-1/2)$ whereas $y_{\max} = 1$. Now let us consider the function $L(\alpha)$. By analogy with the Gaussian function, we define $\alpha_\sigma = \alpha_{\max} \pm 1\sigma$ as the value of α such that $L(\alpha_\sigma) = L(\alpha_{\max}) \times \exp(-1/2)$. Bearing in mind that our function $\mathcal{L}$ is $\ln(L)$, we have $\mathcal{L}(\alpha_\sigma) = \mathcal{L}(\alpha_{\max}) - 1/2$. Therefore, α_σ is the value of α, such that $\mathcal{L}(\alpha)$ is equal to the maximum value $-1/2$. The errors are then $\sigma_+ = \alpha(\mathcal{L}_{\max} - 1/2)_+ - \alpha(\mathcal{L}_{\max})$ and $\sigma_- = \alpha(\mathcal{L}_{\max}) - \alpha(\mathcal{L}_{\max} - 1/2)_-$, where the $+$ and $-$ designate larger and smaller values of α, respectively (Lyons, 1986).

References

Allen, R.L., Bernstein, G.M., Malhotra, R., 2001. The edge of the Solar System. Astrophys. J. 549, L241–L244.

Allen, R.L., Bernstein, G.M., Malhotra, R., 2002. Observational limits on a distant cold Kuiper belt. Astron. J. 124, 2949–2954.

Benz, W., Asphaug, E., 1999. Catastrophic disruptions revisited. Icarus 142, 5–20.

Bottke Jr., W.F., Jedicke, R., Morbidelli, A., Petit, J.-M., Gladman, B., 2000. Understanding the distribution of near-Earth asteroids. Science 288, 2190–2194.

Bottke Jr., W.F., Morbidelli, A., Jedicke, R., Petit, J.-M., Levison, H.F., Michel, P., Metcalfe, T.S., 2002. Debiased orbital and absolute magnitude distribution of the near-Earth objects. Icarus 156, 399–433.

Bottke Jr., W.F., Morbidelli, A., Jedicke, R., Stuart, J.S., Evans, J.B., Stokes, G., 2004. Investigating the near-Earth object population using numerical integration methods and LINEAR data. Bull. Am. Astron. Soc. 36, 1141. [32, 18].

Brandt, J.C., A'Hearn, M.F., Randall, C.E., Schleicher, D.G., Shoemaker, E.M., Stewart, A.I.F., 1996. On the existence of small comets and their interactions with planets. Earth Moon Planets 72, 243–249.

Chen, J., Jewitt, D., 1994. On the rate at which comets split. Icarus 108, 265–271.

Fernández, J.A., 2005. Comets. Nature, Dynamics, Origin and their Cosmogonical Relevance. Springer-Verlag, Dordrecht, The Netherlands.

Fernández, J.A., Tancredi, G., Rickman, H., Licandro, J., 1999. The population, magnitudes, and sizes of Jupiter family comets. Astron. Astrophys. 352, 327–340.

Fernández, J.A., Gallardo, T., Brunini, A., 2002. Are there many inactive Jupiter-family comets among the near-Earth asteroid population? Icarus 159, 358–368.

Ferrín, I., 2005. Secular light curve of Comet 28P/Neujmin 1 and of spacecraft target Comets 1P/Halley, 9P/Tempel 1, 19P/Borrelly, 21P/Giacobinni–Zinner, 26P/Grigg–Skjellerup, 67P/Churyumov–Gerasimenko, and 81P/Wild 2. Icarus 178, 493–516.

Helin, E., Bus, S.J., 1978. IAU Circ. 3271.

Hughes, D.W., 2002. The magnitude distribution and evolution of short-period comets. Mon. Not. R. Astron. Soc. 336, 363–372.

Ivezić, Ž., and 32 colleagues, 2001. Solar System objects observed in the Sloan Digital Sky Survey Commissioning Data. Astron. J. 122, 2749–2784.

Jedicke, R., Metcalfe, T.S., 1998. The orbital and absolute magnitude distributions of main belt asteroids. Icarus 131, 245–260.

Jedicke, R., Larsen, J., Spahr, T., 2002. Observational selection effects in asteroid surveys. In: Bottke, W.F., Paolicchi, P., Binzel, R.P., Cellino, A. (Eds.), Asteroids III. Univ. of Arizona Press, Tucson, pp. 71–87.

Jewitt, D., 2006. Comet D/1819 W1 (Blanpain): Not dead yet. Astron. J. 131, 2327–2331.

Kresák, L., 1978. Passages of comets and asteroids near the Earth. Bull. Astron. Inst. Czech. 29, 103–114.

Kresák, L., Kresáková, M., 1989. The absolute magnitudes of periodic comets. Bull. Astron. Inst. Czech. 40, 269–284.

Kresák, L., Kresáková, M., 1994. Updating the catalogue of absolute magnitudes of periodic comets. Planet. Space Sci. 42, 199–204.

Lamy, P.L., Toth, I., Fernández, Y.R., Weaver, H.A., 2004. The sizes, shapes, albedos, and colors of cometary nuclei. In: Festou, M., Keller, H.U., Weaver, H. (Eds.), Comets II. Univ. of Arizona Press, Tucson, pp. 223–264.

Levison, H.F., Duncan, M.J., 1997. From the Kuiper belt to Jupiter-family comets: The spatial distribution of ecliptic comets. Icarus 127, 13–32.

Lyons, L., 1986. Statistics for Nuclear and Particle Physicists. Cambridge Univ. Press, Cambridge. pp. 85–98.

Meech, K.J., Hainaut, O.R., Marsden, B.G., 2004. Comet nucleus size distributions from HST and Keck telescopes. Icarus 170, 463–491.

Meisel, D.D., Morris, C.S., 1982. Comet head photometry: Past, present, and future. In: Wilkening, L.L. (Ed.), Comets. Univ. of Arizona Press, Tucson, pp. 413–432.

Morbidelli, A., Brown, M.E., 2004. The Kuiper belt and the primordial evolution of the Solar System. In: Festou, M., Keller, H.U., Weaver, H. (Eds.), Comets II. Univ. of Arizona Press, Tucson, pp. 175–191.

Morbidelli, A., Nesvorný, D., Bottke, W.F., Michel, P., Vokrouhlický, D., Tanga, P., 2003. The shallow magnitude distribution of asteroid families. Icarus 162, 328–336.

Pan, M., Sari, R., 2005. Shaping the Kuiper belt size distribution by shattering large but strengthless bodies. Icarus 173, 342–348.

Press, W.H., Teukolsky, S.A., Vetterling, W.T., Flannery, B.P., 1992. Numerical Recipes. Cambridge Univ. Press, Cambridge.

Rickman, H., Fernández, J.A., Gustafson, B.A.S., 1990. Formation of stable dust mantles on short-period comet nuclei. Astron. Astrophys. 237, 524–535.

Sekanina, Z., Yeomans, D.K., 1984. Close encounters and collisions of comets with the Earth. Astron. J. 89, 154–161.

Stuart, J.S., 2001. A near-Earth asteroid population estimate from the LINEAR survey. Science 294, 1691–1693.

Tancredi, G., Fernández, J.A., Rickman, H., Licandro, J., 2000. A catalog of observed nuclear magnitudes of Jupiter family comets. Astron. Astrophys. Suppl. Ser. 146, 73–90.

Tancredi, G., Fernández, J.A., Rickman, H., Licandro, J., 2006. Nuclear magnitudes and size distribution of Jupiter family comets. Icarus 182, 527–549.

Toth, I., 2006. Connections between asteroids and cometary nuclei. In: Ferraz-Mello, S., Lazzaro, D., Fernández, J.A. (Eds.), Asteroids Comets, Meteors, 2005. In: IAU Symp., vol. 229. Cambridge Univ. Press, Cambridge, pp. 67–96.

Trujillo, C.A., Brown, M.E., 2001. The radial distribution of the Kuiper belt. Astrophys. J. 554, 95–98.

Weissman, P.R., Lowry, S.C., 2003. The size distribution of Jupiter-family cometary nuclei. Lunar Planet. Sci. 34.

Whipple, F.L., 1978. Cometary brightness variation and nucleus structure. Moon Planets 18, 343–359.

Whitman, K., Morbidelli, A., Jedicke, R., 2006. The size-frequency distribution of dormant Jupiter-family comets. Icarus 183, 101–114.

Zahnle, K., Schenk, P., Levison, H., Dones, L., 2003. Cratering rates in the outer Solar System. Icarus 163, 263–289.